J Electr Eng Technol Vol. 8, No. 2: 271-281, 2013
http://dx.doi.org/10.5370/JEET.2013.8.2.271

ISSN(Print) 1975-0102
ISSN(Online) 2093-7423

An Improved Poincaré-like Carleman Linearization Approach for Power System Nonlinear Analysis

Zhou-Qiang Wang*, Qi Huang† and Chang-hua Zhang**

Abstract – In order to improve the performance of analysis, it is important to consider the nonlinearity in power system. The Carleman embedding technique (linearization procedure) provides an effective approach in reduction of nonlinear systems. In the approach, a group of differential equations in which the state variables are formed by the original state variables and the vector monomials one can build with products of positive integer powers of them, is constructed. In traditional Carleman linearization technique, the tensor matrix is truncated to form a square matrix, and then regular linear system theory is used to solve the truncated system directly. However, it is found that part of nonlinear information is neglected when truncating the Carleman model. This paper proposes a new approach to solve the problem, by combining the Poincaré transformation with the Carleman linearization. Case studies are presented to verify the proposed method. Modal analysis shows that, with traditional Carleman linearization, the calculated contribution factors are not symmetrical, while such problems are avoided in the improved approach.

Keywords: Carleman embedding, Poincaré transformation, Nonlinear analysis, Power system

1. Introduction

Due to the large scale interconnection of power network and the increase of nonlinear devices (such as power electronic devices), the effective analysis of modern power system is becoming more and more difficult. It is shown that the nonlinear effect should not be neglected, and quite a lot of researches are conducted to deal with this issue, e.g., normal form and modal series [1-3], or other nonlinear analysis methods are developed to perform higher order modal analysis of nonlinear power system model. However, these methods still deal with the state equations of original model, in which the complex nonlinear system theory has to be used. The Carleman embedding technique [4-6], on the other hand, by embedding the new variables formed by all the monomials one can build with products of positive integer powers of the original state variables, replaces the original nonlinear model with an infinite-dimensional linear model. Such an equivalent model can be truncated to be finite-dimensional linear system with an upper triangular square matrix. Therefore, linear theory can be directly applied.

In current available approach, when truncating the Carleman model, it is inevitable that part of nonlinear information is lost. This paper proposes a novel approach, in which the Poincaré transformation approach is introduced to deal with the Carleman linearization system, in an effort to solve this issue.

The effects of the algorithms are evaluated by numerical simulations. The evaluation is accomplished by comparing the approximate solutions, as well as their contribution factors, with the true solution by using Prony analysis. To facilitate the comparison, the indices proximity measures and SNR (Signal Noise Ratio), are defined to ensure that the Prony results best fit the true solution.

The paper is organized as follows. In section 2, the Carleman embedding technique and its truncated linearization and linear analysis are briefly reviewed. Section 3 deduces the solution of the Carleman model with the Poincaré transformation method. Section 4 defines the second-order contribution factors according to the linear contribution factor, and the indices SNR and proximity measures, for quantifying the trajectories of state variables. In section 5, two test systems are used to compare the traditional Carleman linear method with the proposed approach. At the end, the second-order contribution factors of the both solutions are discussed further. Section 6 concludes the paper.

2. Review of Carleman Linear Analysis

2.1 Carleman Embedding Technique

Consider a power system modeled as:

† Corresponding Author: Sichuan Provincial Key Lab of Power System Wide-area Measurement and Control, University of Electronic Science and Technology of China (UESTC), Chengdu, Sichuan China. (hwong@uestc.edu.cn)

* Sichuan Provincial Key Lab of Power System Wide-area Measurement and Control, University of Electronic Science and Technology of China (UESTC), Chengdu, Sichuan China./Dept. of Electrical Engineering, Sichuan Engineering Technical College (SCETC), Deyang, Sichuan China

** Sichuan Provincial Key Lab of Power System Wide-area Measurement and Control, University of Electronic Science and Technology of China (UESTC), Chengdu, Sichuan China.

Received: July 14, 2012; Accepted: October 9, 2012

$$\dot{\mathbf{X}} = \mathbf{f}(\mathbf{X}) \tag{1}$$

where, $\mathbf{X} = [x_1, x_2, \cdots x_n]^{\mathrm{T}} \in R^n$ is the n dimensional state vector and $\boldsymbol{X}_0 = \boldsymbol{X}(0)$. $\boldsymbol{f}$: $R^n \to R^n$ is a smooth vector field and $\mathbf{f}(\mathbf{X}) = [f_1(\mathbf{X}), f_2(\mathbf{X}), \cdots f_n(\mathbf{X})]^{\mathrm{T}}$.

One can expand Eq. (1) by performing a Taylor series in the neighborhood of a stable equilibrium point $\mathbf{X}_{SEP}$, and use again $\mathbf{X}$ as the new state vector to denote $\mathbf{X} - \mathbf{X}_{SEP}$. The Taylor series expansion is

$$\dot{\mathbf{X}} = \mathbf{A}_1\mathbf{X} + \mathbf{A}_2(\mathbf{X} \otimes \mathbf{X}) + \mathbf{A}_3(\mathbf{X} \otimes \mathbf{X} \otimes \mathbf{X}) + \cdots \tag{2}$$

where, system matrix $\mathbf{A}_1 = [\partial \mathbf{f} / \partial \mathbf{X}]_{\mathbf{X}_{SEP}}$ is the $n \times n$ dimension Jacobian matrix. $\mathbf{A}_2$ is the $n \times n^2$ dimension Hessian matrix [3, 6], $\mathbf{A}_3$ is the tensor of the $n \times n^3$ dimension. $\boldsymbol{X}$ belongs to the convergence domain of Taylor series. The symbol $\otimes$ denotes the Kronecker product. We introduce the notation:

$$\mathbf{X}^{[k]} = \underbrace{\mathbf{X} \otimes \mathbf{X} \otimes \cdots \otimes \mathbf{X}}_{k-times} \in R^{m_k}, \; k=1,2,\ldots. \tag{3}$$

Then, the Eq. (2) can be rewritten as:

$$\dot{\mathbf{X}} = \sum_{k=1}^{\infty} \mathbf{A}_k \mathbf{X}^{[k]} \tag{4}$$

where, the $\mathbf{A}_k \in R^{n \times m_k}$, $m_k \triangleq \binom{n+k-1}{k}$, $k=1,2,\ldots..$, are the matrix valued functions.

In the Carleman embedding technique [4, 6], the power series representation (4) is first truncated to N. Then truncated system is:

$$\dot{\mathbf{X}} = \sum_{k=1}^{N} \mathbf{A}_k \mathbf{X}^{[k]} \tag{5}$$

Define the time derivative of j-th Kronecker product:

$$\frac{d(\mathbf{X}^{[j]})}{dt} = \frac{d\left(\underbrace{\mathbf{X} \otimes \mathbf{X} \otimes \cdots \otimes \mathbf{X}}_{j-times}\right)}{dt} = \sum_{k=1}^{N-j+1} (\mathbf{A}_k \otimes \underbrace{\mathbf{I}_n \otimes \cdots \otimes \mathbf{I}_n}_{(j-1)times}$$
$$+ \mathbf{I}_n \otimes \mathbf{A}_k \otimes \mathbf{I}_n \otimes \cdots \otimes \mathbf{I}_n + \mathbf{I}_n \otimes \cdots \otimes \mathbf{I}_n \otimes \mathbf{A}_k)\mathbf{X}^{[k+j-1]}$$
$$\triangleq \sum_{k=1}^{N-j+1} (\mathbf{A}_k^j)\mathbf{X}^{[k+j-1]} \tag{6}$$

where, $\mathbf{A}_k^1 = \mathbf{A}_k$ for j =1, and for j >1

$$\mathbf{A}_k^j = \mathbf{A}_k \otimes \underbrace{\mathbf{I}_n \otimes \cdots \otimes \mathbf{I}_n}_{(j-1)times} + \mathbf{I}_n \otimes \mathbf{A}_k \otimes \mathbf{I}_n \otimes \cdots \otimes \mathbf{I}_n$$
$$+ \cdots + \mathbf{I}_n \otimes \cdots \otimes \mathbf{I}_n \otimes \mathbf{A}_k$$

And then define the vectors of Kronecker-products as a new vector field:

$$\mathbf{X}^{\otimes} \triangleq [\mathbf{X}, \mathbf{X}^{[2]}, \cdots, \mathbf{X}^{[j]}, \cdots]^T \tag{7}$$

where, $\dim(\mathbf{X}^{\otimes}) = M = n + m_2 + \cdots + m_N$

Then, a truncated Carleman linearization of original state Eq. (1) can be obtained:

$$\dot{\mathbf{X}}^{\otimes} = \mathbf{A}^{\otimes}\mathbf{X}^{\otimes} \tag{8}$$

where,

$$\mathbf{A}^{\otimes} = \begin{bmatrix} \mathbf{A}_1^1 \mathbf{A}_2^1 \cdots \mathbf{A}_N^1 \\ \mathbf{0} \; \mathbf{A}_1^2 \cdots \mathbf{A}_{N-1}^2 \\ \vdots \; \vdots \; \ddots \; \vdots \\ \mathbf{0} \; \mathbf{0} \; \mathbf{0} \; \mathbf{A}_1^N \end{bmatrix} \in R^{\sum_{r=1}^{N} n^r \times \sum_{r=1}^{N} n^r}$$

And the matrix $\mathbf{A}_1^1$ is exactly the matrix defined in (2).

2.2 Modal analysis of carleman linearization

The matrix $\mathbf{A}^{\otimes}$ is a $\sum_{r=1}^{N} n^r \times \sum_{r=1}^{N} n^r$ dimension upper triangular matrix, and the eigenvalues can be obtained by

$$\left|\lambda I - \mathbf{A}^{\otimes}\right| = \left|\lambda^1 I - \mathbf{A}_1^1\right| \left|\lambda^2 I - A_1^2\right| \cdots \left|\lambda^N I - A_1^N\right| = \mathbf{0} \tag{9}$$

Solving the above equation, the eigenvalues of the system can be obtained,

$$eig(\mathbf{A}^{\otimes}) = \mathbf{\Lambda}^{\otimes} = \begin{bmatrix} J(\lambda^1) & & & \\ & J(\lambda^2) & & \\ & & \ddots & \\ & & & J(\lambda^N) \end{bmatrix} \tag{10}$$

where,

$$J(\lambda^1) = diag([\lambda_1, \lambda_2, \cdots, \lambda_n])$$
$$J(\lambda^2) = diag([\lambda_1 + \lambda_1, \lambda_1 + \lambda_2, \cdots, \lambda_n + \lambda_n])$$
$$J(\lambda^N) = diag(\{\lambda_{k_1} + \lambda_{k_2} + \cdots + \lambda_{k_n}\})$$
$$k_1, k_2, \cdots, k_n = 1,2,\ldots\ldots,n$$

It is shown that the eigenvalue space of Carleman linear model is formed by the eigenvalues from the linear space of the matrix $\mathbf{A}_1^1$, $\mathbf{A}_1^2$ and the matrix $\mathbf{A}_1^N$, which contain eigenvalues associated with the higher-order modal interaction.

In this paper, to reduce the complexity in the deduction, only N =2 is considered. However, the developed methods here applies for N >2 cases. Suppose $\mathbf{U}^{\otimes}$ and $\mathbf{V}^{\otimes}$ are the matrices of the right and left eigenvectors of $\mathbf{A}^{\otimes}$, respectively. In linear theory, taking similar transform and inverse transform with $\mathbf{X}^{\otimes} = \mathbf{U}^{\otimes}\mathbf{Y}^{\otimes}$, the free response of system (8) is:

$$\mathbf{X}^{\otimes} = \mathbf{U}^{\otimes} e^{\Lambda^{\otimes} t} \mathbf{V}^{\otimes}\mathbf{X}^{\otimes}(\mathbf{0}) \tag{11}$$

and the analytical solutions is [6]:

$$x_i(t) = \sum_{j=1}^{n} u_{ij}^{\otimes} c_j^1 e^{\lambda_j^1 t} + \sum_{k=n+1}^{n+n^2} u_{ik}^{\otimes} c_k^2 e^{\lambda_k^2 t} \tag{12}$$

where,

$$c_j^1 = \sum_{p=1}^{n+n^2+n^3} v_{jp}^{\otimes} x_p^0 \quad j = 1,2,\ldots\ldots,n$$

$$c_k^2 = \sum_{q=1}^{n+n^2+n^3} v_{kq}^{\otimes} x_q^0 \quad k = n+1, n+2, \ldots\ldots, n+n^2$$

In which, $\lambda_j^1 = \lambda_1, \lambda_2, ..., \lambda_n$ are the first-order modes eigenvalues, and $\lambda_k^2 = \lambda_1 + \lambda_1, \lambda_1 + \lambda_2, ..., \lambda_n + \lambda_n$ are the second-order combined eigenvalues arising from the modal interaction of the linear modes eigenvalues. The $u_{ij}^{\otimes}, u_{ik}^{\otimes} \in \mathbf{U}^{\otimes}$ are the eigenvectors corresponding to the eigenvalues λ_j^1, λ_k^2. $x_p^0, x_q^0 \in \mathbf{X}^{\otimes}(\mathbf{0})$ are the initial condition.

3. Solving the Truncated Carleman Linearized Model by Poincaré Transformation

Reconsider (8) and (12), it is found that the higher-order terms $\mathbf{A}_k^1$ have been replaced by $\mathbf{A}_1^k$ in the process of obtaining eigenvalues and solution. In other words, the 2nd order combined eigenvalues belong to $\mathbf{A}_1^2$ but do not belong to $\mathbf{A}_2^1$. In order to include the ignored higher order terms, system (8) is split into:

$$\dot{\mathbf{X}}^{\otimes} = \mathbf{A}_S^{\otimes} \mathbf{X}^{\otimes} + \mathbf{A}_{N2}^{\otimes} \mathbf{X}^{\otimes} + \cdots \tag{13}$$

where,

$$\mathbf{A}_S^{\otimes} = \begin{bmatrix} \mathbf{A}_1^1 & \mathbf{0} \\ \mathbf{0} & \mathbf{A}_1^2 \end{bmatrix}, \quad \mathbf{A}_{N2}^{\otimes} = \begin{bmatrix} \mathbf{0} & \mathbf{A}_2^1 \\ \mathbf{0} & \mathbf{0} \end{bmatrix}$$

The state-space equation for the *i*-th state variable of *j*-th order is given by

$$\dot{x}_i^{[j]} = A_i^j \mathbf{X}^{[j]} + H_2^{ji}(\mathbf{X}^{[j]} \otimes \mathbf{X}) \tag{14}$$

where, A_i^j is the *j*-th order and *i*-th row of the $\mathbf{A}_S^{\otimes}$. H_2^{ji} is the *j*-th order and *i*-th row element of the $\mathbf{A}_{N2}^{\otimes}$.

Suppose $\mathbf{U}^{\otimes}$ and $\mathbf{V}^{\otimes}$ are the matrices of the right and left eigenvectors of $\mathbf{A}_S^{\otimes}$, respectively. The state Eq. (13) in *y*-coordinates, after performing a $\mathbf{X}^{\otimes} = \mathbf{U}^{\otimes}\mathbf{Y}^{\otimes}$ coordinate transformation, is

$$\dot{\mathbf{Y}}^{\otimes} = \mathbf{\Lambda}^{\otimes}\mathbf{Y}^{\otimes} + \mathbf{V}^{\otimes}\mathbf{A}_{N2}^{\otimes}\mathbf{U}^{\otimes}\mathbf{Y}^{\otimes} + \cdots \tag{15}$$

where, $\mathbf{\Lambda}^{\otimes} = diag(J_{\lambda_{k_1}}, J_{\lambda_{k_1}+\lambda_{k_2}}, \cdots, J_{\lambda_{k_1}+\lambda_{k_2}+\cdots+\lambda_{k_j}}, \cdots)$, the *j-th* order state equations for Jordan form variables are :

$$\dot{y}^{[j]} = J(\lambda^j) y^{[j]} + \mathbf{V}^{\otimes} \begin{bmatrix} H_2^{j1}(U^{[j]} \otimes U)(y^{[j]} \otimes y) \\ H_2^{j2}(U^{[j]} \otimes U)(y^{[j]} \otimes y) \\ \cdots \\ H_2^{jn^j}(U^{[j]} \otimes U)(y^{[j]} \otimes y) \end{bmatrix} \tag{16}$$

where, the *m-th* state equations are :

$$\dot{y}_m^{[j]} = \lambda_m^j y_m^{[j]} + \sum_{k=1}^{n}\sum_{l=1}^{n} C_{kl}^{m\otimes} y_k^{[j]} y_l + \cdots\cdots \tag{17}$$

where, $C_{kl}^{m\otimes}$ is the klth element of the matrix

$$C^{m\otimes} = \frac{\mathbf{1}}{\mathbf{2}} \sum_{p=1}^{n^j} v_{mp}^{\otimes} [H_2^{jP}(U^{[j]} \otimes U)] = [C_{kl}^{m\otimes}].$$

The term in the brackets is an n^j-by-n^{j+1} matrix; $v_{mp}^{\otimes}$ is the *mp*-th element of the matrix $\mathbf{V}^{\otimes}$.

Introducing a new vector field $\mathbf{Z} = [z_1, z_2, \cdots z_n]^T$ and $\mathbf{Z}^{\otimes} = [\mathbf{Z}, \mathbf{Z}^{[2]}, \cdots, \mathbf{Z}^{[j]}, \cdots]^T$, and using the Poincaré transformation $\mathbf{Y}^{\otimes} = \mathbf{Z}^{\otimes} + \mathbf{h}_2(\mathbf{Z}^{\otimes})$ [7], the above equation can be rewritten as:

$$\dot{\mathbf{Z}}^{\otimes} = \mathbf{\Lambda}^{\otimes}\mathbf{Z}^{\otimes} + F_2(\mathbf{Z}^{\otimes}) + \cdots = \mathbf{\Lambda}^{\otimes}\mathbf{Z}^{\otimes} + \sum_{k=1}^{\infty} F_k(\mathbf{Z}^{\otimes}) \tag{18}$$

where,

$$F_k(\mathbf{Z}^{\otimes}) = \mathbf{V}^{\otimes}\mathbf{A}_{Nk}^{\otimes}\mathbf{U}^{\otimes}\mathbf{Z}^{\otimes} + \mathbf{\Lambda}^{\otimes} h_k(\mathbf{Z}^{\otimes}) - Dh_k(\mathbf{Z}^{\otimes})\mathbf{\Lambda}^{\otimes}\mathbf{Z}^{\otimes} \tag{19}$$

Examination of (18) suggests that in order to remove the higher order terms, one can introduce a linear operator $L_{\mathbf{A}}$ on function h_k to form the homological equation:

$$L_{\mathbf{A}} h_k(\mathbf{y}) = Dh_{\mathbf{k}}(\mathbf{Z}^{\otimes})\mathbf{\Lambda}^{\otimes}\mathbf{Z}^{\otimes} - \mathbf{\Lambda}^{\otimes} h_{\mathbf{k}}(\mathbf{Z}^{\otimes}) \tag{20}$$

The solution of the homological equation can be obtained if and only if $\sum_{l=1}^{n} m_l \lambda_l^{k+j-1} - \lambda_i \neq \mathbf{0}$. The approximate solution of system in *z*-coordinates is a set of decoupled linear differential equations:

$$\dot{\mathbf{Z}}^{\otimes} = \mathbf{\Lambda}^{\otimes}\mathbf{Z}^{\otimes}; \quad \dot{\mathbf{Z}}^{[j]} = \mathbf{\Lambda}^{[j]}\mathbf{Z}^{[j]}; \quad \dot{z}_m^j = \lambda_m^j z_m^j \tag{21}$$

The solution of z_m^j and y_m^j is:

$$z_m^j(t) = e^{\lambda_m^j t} z_{m\mathbf{0}}^j \tag{22}$$

$$y_m^j = z_m^j + \sum_{k=1}^{n}\sum_{l=1}^{n} h\mathbf{2}_{kl}^m z_k^j z_l \tag{23}$$

where, $h\mathbf{2}_{kl}^m = \dfrac{C_{kl}^{m\otimes}}{\lambda_k^j + \lambda_l - \lambda_j}$, $\lambda_k^j + \lambda_l \neq \lambda_j$.

With the inverse transform $\mathbf{X}^{\otimes} = \mathbf{U}^{\otimes}\mathbf{Y}^{\otimes}$, the solution of x_i^j is:

$$x_i^j(t)=\sum_{m=1}^{n^j} u_{im}^{\otimes} z_{m0}^j e^{\lambda_m^j t} + \sum_{m=1}^{n^j} u_{im}^{\otimes} \sum_{k=1}^{n}\sum_{l=1}^{n} h\mathbf{2}_{kl}^m z_{k0}^j z_{l0} e^{(\lambda_k^j+\lambda_l)t}$$
$$m = 1,2,\ldots,n \ ; \ j = 1,2,\ldots,N \ ; \ i = 1,2,\ldots, n^j \qquad (24)$$

where, the symbols $\lambda_m^{\mathbf{1}}, \lambda_m^{\mathbf{2}}$ and $u_{im}^{\otimes}$ are the same as above. The initial condition z_{m0}^j of $z_m^j(t)$ can be computed by solving the nonlinear equations $\mathbf{Y}_0^{\otimes} = \mathbf{Z}_0^{\otimes} + \mathbf{h}_2(\mathbf{Z}_0^{\otimes})$.

4. Quantitative Comparison of the Responses

4.1 Nonlinear contribution factors

In a linear system, the solution of a state variable is:

$$x_i(t)=\sum_{j=1}^{n} u_{ij} y_{j0} e^{\lambda_j t} = \sum_{j=1}^{n} \sigma_{ij} e^{\lambda_j t} \qquad (25)$$

The term $\sigma_{ij}=u_{ij}y_{j0}$ are referred to as "linear contribution factors", describing the contribution of the *j*-th mode in the oscillations of the state *i* for a given disturbance.

Comparing the solution (25), (12) and (24), the second order solutions given in (12) and (24) may be rewritten as:

$$x_i(t) = \sum_{j=1}^{n} \sigma_{ij}^{\mathbf{1}} e^{\lambda_j^{\mathbf{1}} t} + \sum_{k=n+1}^{n+n^2} \sigma_{ik}^{\mathbf{2}} e^{\lambda_k^{\mathbf{2}} t} \qquad (26)$$

$$x_i^j(t)=\sum_{m=1}^{n^j} \sigma_{\mathbf{2}im} e^{\lambda_m^j t} + \sum_{k=1}^{n}\sum_{l=1}^{n} \sigma_{\mathbf{22}ikl} e^{(\lambda_k^j+\lambda_l)t} \qquad (27)$$

Here, $\sigma_{ij}^{\mathbf{1}} = u_{ij}^{\otimes} c_j^{\mathbf{1}}$ and $\sigma_{ik}^{\mathbf{2}} = u_{ik}^{\otimes} c_k^{\mathbf{2}}$, $\sigma_{\mathbf{2}im} = u_{im}^{\otimes} z_{m0}^j$ and $\sigma_{\mathbf{22}ikl} = \sum_{m=1}^{n^j} u_{im}^{\otimes} h\mathbf{2}_{kl}^m z_{k0}^j z_{l0}$. Thus, the second-order contribution factors are defined in a manner very similar to the linear contribution factors described above. Note that there are two types of second-order contribution factors. The first type of the second-order contribution factors, $\sigma_{ij}^{\mathbf{1}}$ or $\sigma_{\mathbf{2}im}$, gives the contribution of the mode $\lambda_j^{\mathbf{1}}$ or λ_m^j to the response of the state *i*. It's clear that the linear contribution factor σ_{ij} is a part of $\sigma_{ij}^{\mathbf{1}}$ or $\sigma_{\mathbf{2}im}$. The second type of the second-order contribution factors, $\sigma_{ik}^{\mathbf{2}}$ or $\sigma_{\mathbf{22}ikl}$, gives the contributions of the combination modes $\lambda_k^{\mathbf{2}}$ or $\lambda_k^j + \lambda_l$ to the response of state *i*.

4.2 Comparing with results from prony

In order to compare the accuracy of the solutions obtained from different methods, the contribution of a mode in an approximate solution is compared with that obtained by performing Prony analysis on the true responses.

Suppose the solution $x(n)$ is the discrete form of the SBS (Step by Step) solution $x(t)$ of original system (1). And the Prony fitted response of original system (1) can be written as follows [8]:

$$\hat{x}(n) = \sum_{i=1}^{p} \tilde{A}_i e^{j\theta_i} e^{\lambda_i \Delta t} \ ; \ \ \lambda_i = \alpha_i + j\mathbf{2}\pi f_i \qquad (28)$$

Thus, the exponential modes, containing the frequency f_i, the amplitude $\tilde{A}_i$, the attenuation factor α_i and the phase θ_i, can be obtained.

The solutions (26) and (27) consist of a sum of weighted exponential oscillations, where the weights are the contribution factors. The frequencies of oscillation are determined by the imaginary parts of the eigenvalues λ. Therefore, the exponential modes obtained by Prony analysis can be regarded as a reference when comparing the contribution factors in linear method, traditional Carleman linear method and the proposed method. For example, σ_{ij}, $(\sigma_{ij}^{\mathbf{1}}, \sigma_{ik}^{\mathbf{2}})$, $(\sigma_{\mathbf{2}im}, \sigma_{\mathbf{22}ikl})$ can be compared with $\tilde{A}_i$ under the same frequency f_i or λ_i in the response (25), (26) and (27).

In order to ensure the accuracy of Prony's fitting curve, the *SNR* based on Root Mean Square and proximity measure are introduced [9]:

$$SNR = -\mathbf{20}\log\left(\sqrt{\frac{\sum_{n=1}^{n_t} |\hat{x}(n)-x(n)|^2}{\sum_{n=1}^{n_t} |x(n)|^2}}\right) \ (\text{dB}) \qquad (29\text{-}1)$$

$$error = \frac{\sum_{n=1}^{n_t} |\hat{x}(n)-x(n)|}{\sum_{n=1}^{n_t} |x(n)|} \times \mathbf{100}\,(\%) \qquad (29\text{-}2)$$

where, n_t is number of data points. A large SNR indicates that the fitting of data in time domain are accurate. A small error indicates that the fitting solution with included higher-order terms is close to the true solution (SBS solution). For general cases, the SNR ≥ 40 dB and error < 10% are considered as a reference to estimate the fitting degree.

5. Case Study and Discussion

5.1 Test system #1

A single-machine infinite bus (SMIB) system ([10, Section 12.3]) shown in Fig. 1 is selected to demonstrate the effect of methods both Carleman linearization and

improved method, with parameters given in the figure. The generator is modeled using three-order model (ω, δ, E'_q), and equipped with a thyristor (one-order fast-response) exciter as excitation system. In analyzing the system oscillation, a three-phase short-circuit-to-ground fault is applied at line CCT2 and cleared in 0.1s. The linear modes of the test system are shown in Table 1.

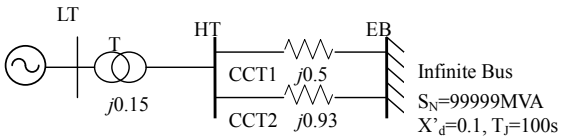

Fig. 1. The SMIB system

Table 1. The system modes of the test system #1

Mode#	EIGENVALUE	Fre.(Hz)	Damp.(%)
1	-19.733181	0	100
2,3	-0.398092±6.756324i	1.075302	5.881939
4	-0.020874	0	100
5	-0.408973	0	100

Figs. 2~5 show the time response of ($\omega, \delta, E'_q, E_{fd}$) in SMIB by four different methods. It is clear that the trajectory of Poincaré transformation combined with Carleman embedding technique (P-Carleman) is closer to the SBS curve than the trajectory of Carleman linearization (linear-Carleman).

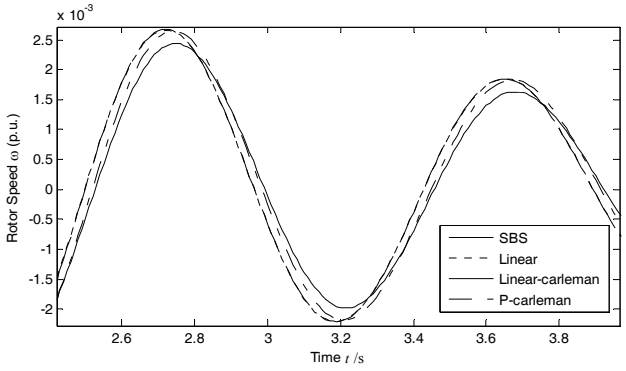

Fig. 2. Time response of ω in SMIB

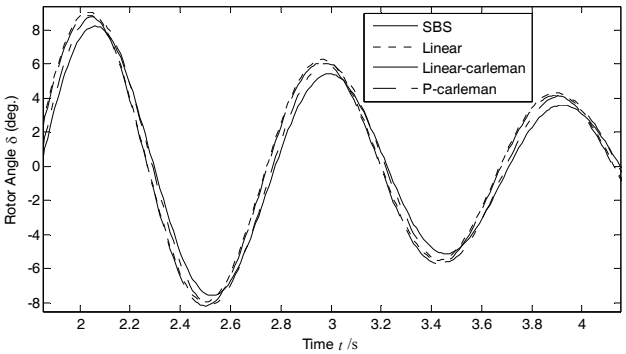

Fig. 3. Time response of δ in SMIB

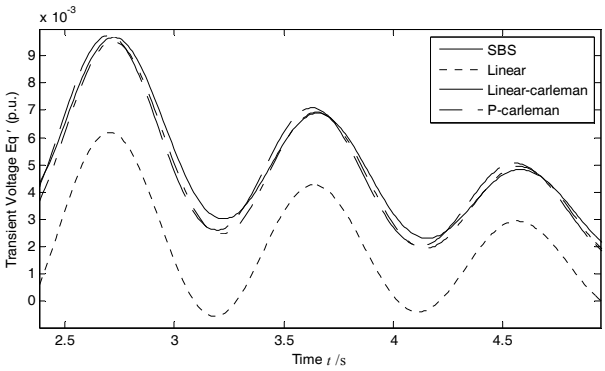

Fig. 4. Time response of E'_q in SMIB

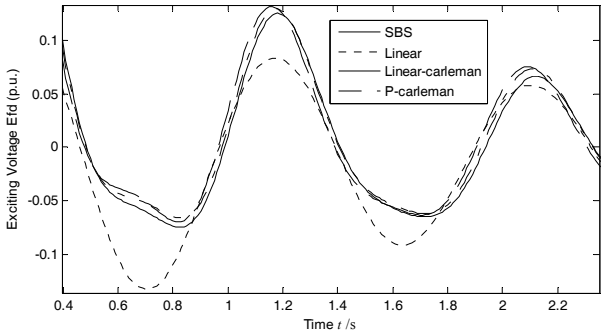

Fig. 5. Time response of E_{fd} in SMIB

In order to compare the accuracy of the both methods, the contribution factors (σ_{ij} , $\sigma^{\mathbf{1}}_{ij}$, $\sigma_{\mathbf{2}im}$) and ($\sigma^{\mathbf{2}}_{ik}$, $\sigma_{\mathbf{22}ikl}$), are respectively listed in descending order in Table 2 and Table 3, whilst the SBS curve of ω and its Prony fitting curve are shown in Fig. 6. In this case, *SNR*=97.66dB and *error* = 0.86%, evidence that the results of Prony analysis are effective. The modes from Prony analysis are listed in Table 4.

Since complex conjugate pairs play a decisive role in the oscillation, they are selected for further consideration here. In Table 2, for any mode, the contribution factors obtained by three methods are almost the same. The only complex conjugate pairs in Table 2, modes 2 and 3, are corresponding to the modes 7 and 8 in Table 4.

$$f_{\lambda_{\mathbf{2(3)}}} = 1.075302(\text{Hz}) \approx f^{\text{Prony}}_{\lambda_{\mathbf{7(8)}}} = 1.074864(\text{Hz})$$

$$\sigma_{ij}(\lambda_{\mathbf{2(3)}}) \approx \sigma^{\mathbf{1}}_{ij}(\lambda_{\mathbf{2(3)}}) \approx \sigma_{\mathbf{2}im}(\lambda_{\mathbf{2(3)}}) \approx \tilde{A}_{\mathbf{7(8)}}$$

In Table 3, the second type of 2nd order contribution factors ($\sigma^{\mathbf{2}}_{ik}$, $\sigma_{\mathbf{22}ikl}$) are listed in descending order. The 2nd order combination modes (2,2) and (3,3), are corresponding to the modes 4 and 5 in Table 4.

$$f_{\lambda_{(\mathbf{2,2})(\mathbf{3,3})}} = 1.075302 \times 2(\text{Hz}) \approx f^{\text{Prony}}_{\lambda_{\mathbf{4(5)}}} = 2.137168(\text{Hz})$$

$$\sigma^{\mathbf{2}}_{ik}(\lambda_{(\mathbf{2,2})(\mathbf{3,3})}) \approx \sigma_{\mathbf{22}ikl}(\lambda_{(\mathbf{2,2})(\mathbf{3,3})}) \approx \tilde{A}_{\mathbf{4(5)}}$$

A marked difference of the contribution factors of the

2nd order modes (2,5) and (3,5) calculated with different methods occurs in Table 3. Considering their corresponding modes 9 and 10 in Table 4, the comparison can be obtained as:

$$f_{\lambda_{(2,5)(3,5)}} = 1.075302 \text{ (Hz)} \approx f^{Prony}_{\lambda_{9(10)}} = 0.977549(\text{Hz})$$
$$\sigma^2_{ik}(\lambda_{(2,5)(3,5)}) = \mathbf{0.18003\times10^{-3}} \neq \sigma_{22ikl}(\lambda_{(2,5)(3,5)})$$
$$= \mathbf{0.52699\times10^{-3}} = \tilde{A}_{9(10)} = 0.00054451$$

This reveals the 2nd order contribution factors σ_{22ikl} are more accurate and closer to the corresponding modes' contribution in the true solution. In other words, the solution from combined Poincaré transformation method can obtain better results.

Table 2. 1st order contribution factors of ω by 3 methods

Mode*i*	σ_{ij}	σ^1_{ij}	σ_{2im}
1	0.00010994815	0.00010921993	0.00011034864
2,3	0.00393543232	0.00394550970	0.00391870952
4	0.00000146376	0.00000170010	0.00000169795
5	0.00001327590	0.00003948575	0.00003899603

Table 3. 2nd order contribution factors of ω by 2 methods

Mode *ij*	σ^2_{ik} (*10^{-3})	Mode *ij*	σ_{22ikl} (*10^{-3})
(2,5)(3,5)	0.180033561696	(2,5)(3,5)	0.526990527282
(2,3)	0.073591608632	(2,2)(3,3)	0.063209737945
(2,2)(3,3)	0.065019946925	(2,3)	0.051712425053
(1,2)(1,3)	0.005789310134	(1,2)(1,3)	0.005922683228
(2,4)(3,4)	0.002050779958	(1,5)	0.004447825264
(1,5)	0.000923751727	(2,4)(3,4)	0.002368960209
(1,1)	0.000031561947	(5,5)	0.000571100045
(5,5)	0.000023818398	(1,1)	0.000038780642
(1,4)	0.000006278597	(1,4)	0.000014288119
(4,5)	0.000000302655	(4,5)	0.000000219002
(4,4)	0.000000000009	(4,4)	0.000000000031

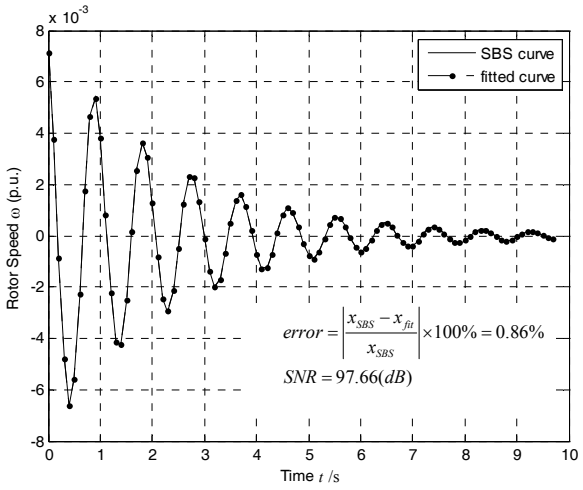

Fig. 6. Prony fitting curve of ω in SMIB

Table 4. Prony results of SBS curve ω (10 orders, *SNR*= 97.66dB, *error* =0.8571%)

Mode *i*	AMPLITUDE	Fre.(Hz)	Attenuation factor	Damp. ratio
1	0.00000086	0.000000	-0.409293	-1.000000
2,3	0.00002342	1.738400	-1.357540	-0.123337
4, 5	0.00006393	2.137618	-0.842109	-0.062576
6	0.00011580	0.000000	-2.997782	-1.000000
7,8	0.00374687	1.074864	-0.414209	-0.061217
9,10	0.00054451	0.977549	-1.286471	-0.205002

5.2 Test system #2

Consider a WSCC-9 (Western System Coordinating Council) power system [11], shown in Fig. 7. The parameters are referred to [12]. A three-phase short-circuit-to-ground fault is applied at Bus GEN1-230 and cleared in 0.15s. There are 4 complex conjugate pairs, as shown in Table 5.

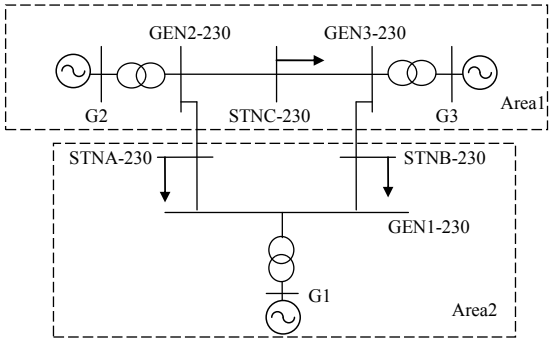

Fig. 7. The WSCC-9 system.

Table 5. The system modes of the test system #2

Mode#	EIGENVALUE	Fre.(Hz)	Damp.(%)
1	-19.060167	0	100
2,3	-0.111826±12.063696i	1.919997	0.926924
4,5	**-0.033345±7.964903i**	**1.267654**	**0.418655**
6,7	-5. 261004±6.770876i	1.077618	61.356026
8,9	-5. 180107±4.787777i	0.761998	73.436953
10	-0.108179	0	100
11	-1.353255	0	100

After the same analysis in the Test System #1, the time response of ($\omega_2, \delta_{21}, E'_{q2}, E_{fd2}$) obtained by the 4 methods are respectively shown in Figs. 8~11. It is shown that P-Carleman solution can get better results.

The contribution factors (σ_{ij}, σ^1_{ij}, σ_{2im}) and (σ^2_{ik}, σ_{22ikl}) are respectively listed in descending order in Table 6 and Table 7, whilst the SBS curve of ω_2 and its Prony fitting curve are shown in Fig. 12. The *SNR*=117.76dB and *error* =0.25%, evidence that the fitting curve and the results of Prony analysis are effective. The modes of Prony analysis are listed in Table 8.

In Table 6, the complex conjugate pairs, modes 2 and 3, are corresponding to the modes 35 and 36 in Table 8, as

well as the modes 4 and 5 corresponding to modes 31 and 32.

$$f_{\lambda_{2(3)}}=1.919997\ \text{(Hz)}\ \approx f^{\Pr ony}_{\lambda_{35(36)}}=1.913633\text{(Hz)}$$
$$\sigma_{ij}(\lambda_{2(3)})=0.001597\ \neq \sigma^{1}_{ij}(\lambda_{2(3)})=0.001997$$
$$\neq \sigma_{2im}(\lambda_{2(3)})=0.001760\ \approx \tilde{A}_{35(36)}=0.001790$$
$$f_{\lambda_{4(5)}}=1.267654\ \text{(Hz)}\approx f^{\Pr ony}_{\lambda_{39(40)}}=1.260021\ \text{(Hz)}$$
$$\sigma^{2}_{ik}(\lambda_{(4,4)(5,5)})=\sigma_{22ikl}(\lambda_{(4,4)(5,5)})\approx \tilde{A}_{31(32)}$$

Note that the numerical value of the first order contribution factors in P-Carleman solution, as in Test System #1, is closest to the reference. The second type of contribution factors about combination modes (2,2), (3,3), (4,4) and (5,5) in Table 7 are corresponding to the modes 21, 22, 31 and 32 in Table 8.

$$f_{\lambda_{(2,2)(3,3)}}=1.919997\times 2\ \text{(Hz)}\ \approx f^{\Pr ony}_{\lambda_{21(22)}}=3.912319\text{(Hz)}$$
$$\sigma^{2}_{ik}(\lambda_{(2,2)(3,3)})\neq \sigma_{22ikl}(\lambda_{(2,2)(3,3)})\approx \tilde{A}_{21(22)}=0.00001654$$
$$f_{\lambda_{(4,4)(5,5)}}=1.267654\times 2\ \text{(Hz)}\approx f^{\Pr ony}_{\lambda_{31(32)}}=2.505604\ \text{(Hz)}$$
$$\sigma^{2}_{ik}(\lambda_{(4,4)(5,5)})\approx \sigma_{22ikl}(\lambda_{(4,4)(5,5)})\approx \tilde{A}_{31(32)}=0.0001255$$

This reveals the contribution factors of these second order dominant modes by the proposed method can approximate to the analytical results of SBS's solution better.

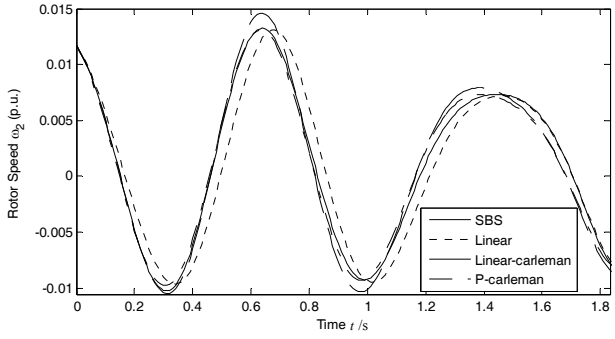

Fig. 8. Time response of ω_2 in WSCC-9

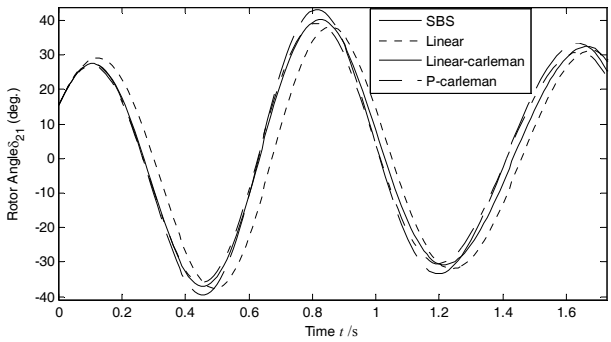

Fig. 9. Time response of δ_{21} in WSCC-9

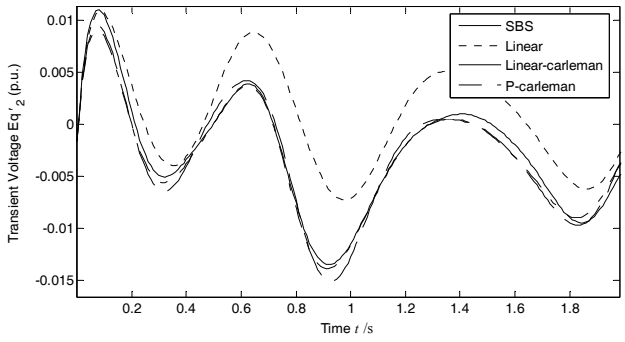

Fig. 10. Time response of E'_{q2} in WSCC-9

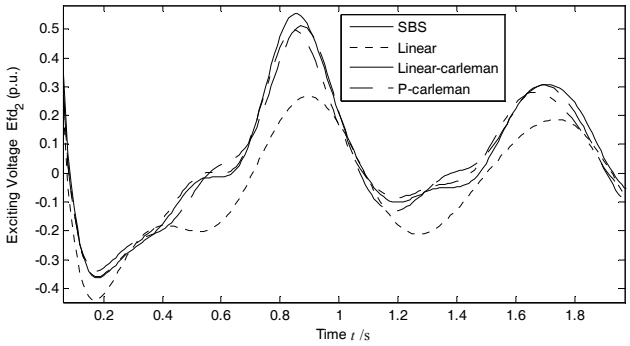

Fig. 11. Time response of E_{fd2} in WSCC-9

Table 6. 1st order contribution factors of ω_2 by 3 methods

Mode$i$	σ_{ij}	σ^{1}_{ij}	σ_{2im}
1	0.00013629248	0.00013523945	0.00013428955
2, 3	0.00159717172	0.00199739074	0.00176072469
4, 5	0.00480099693	0.00512797306	0.00470748315
6, 7	0.00340184486	0.00337565301	0.00319804656
8, 9	0.00027653200	0.00029283114	0.00029094858
10	0.00089714798	0.00910328501	0.00841446193
11	0.00003579549	0.00004219124	0.00004434574

Table 7. 2nd order contribution factors of ω_2 by 2 methods

Mode ij	σ^{2}_{ik}	Mode ij	σ_{22ikl}
(4,5)	0.011062666997	(4,5)	0.010691489092
(2,3)	0.001370322074	(2,3)	0.001646168744
(5,7)(4,6)	0.000572065489	(2,6)(3,7)	0.000589887643
(2,6)(3,7)	0.000571635314	(5,7)(4,6)	0.000521756285
(5,6)(4,7)	0.000522475105	(5,6)(4,7)	0.000460889280
(6,8)(7,9)	0.000459949510	(6,8)(7,9)	0.000453688079
(6,7)	0.000434131788	(2,7)(3,6)	0.000403034301
(2,7)(3,6)	0.000389799079	(6,7)	0.000370910975
(6,6)(7,7)	0.000384518377	(3,9)(2,8)	0.000355072048
(6,9)(7,8)	0.000342744709	(6,9)(7,8)	0.000336614634
(4,8)(5,9)	0.000312403953	(6,6)(7,7)	0.000335715697
(3,9)(2,8)	0.000306230293	(4,8)(5,9)	0.000322395755
(5,8)(4,9)	0.000259130016	(5,8)(4,9)	0.000265566934
(8,9)	0.000221393053	(8,9)	0.000242992678
(3,8)(2,9)	0.000169734618	(3,8)(2,9)	0.000196268451
------	------	------	------
(4,4)(5,5)	0.000124897021	(4,4)(5,5)	0.000121393501
(2,2)(3,3)	0.000014123153	(2,2)(3,3)	0.000017238124

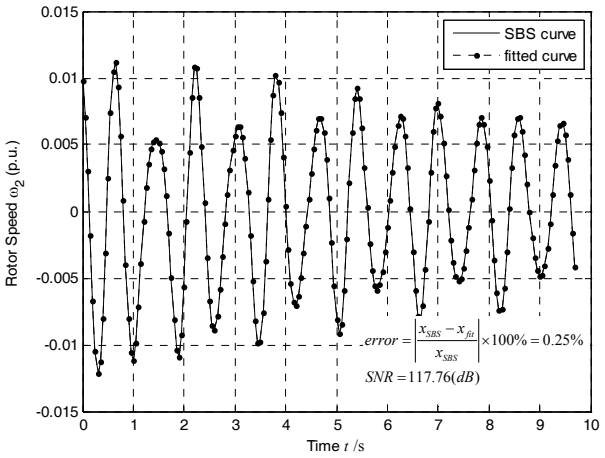

Fig. 12. Prony fitted curve of ω_2 in WSCC-9

Table 8. Prony results of SBS curve ω_2 (49 orders, *SNR*= 114.34dB, *error*=0.2541%)

Mode i	AMPLITUDE	Fre.(Hz)	Attenuation factor	Damp. ratio
1, 2	0.00000050	1.301541	-0.162314	-0.019844
3, 4	0.00000056	0.551010	-0.006102	-0.001762
5	0.00000001	0.000000	-0.629168	-1.000000
6	0.00000839	0.000000	-1.994287	-1.000000
7, 8	0.00000056	0.893122	-0.311967	-0.055507
9,10	0.00000161	1.664609	-0.574859	-0.054880
11,12	0.00000149	2.025568	-0.343341	-0.026968
13,14	0.00000203	2.359376	-0.200662	-0.013535
15, 16	0.00000145	2.611001	-0.227443	-0.013863
17,18	0.00001760	3.258839	-0.574378	-0.028040
19,20	0.00000376	3.415605	-0.256717	-0.011961
21,22	0.00001654	3.912319	-0.276250	-0.011237
23,24	0.00000566	3.800176	-0.069553	-0.002913
25,26	0.00005173	3.716064	-0.608358	-0.026046
27,28	0.00005128	3.170452	-0.193052	-0.009691
29,30	0.00075967	2.984969	-5.128878	-0.263780
31,32	0.00012550	2.505604	-0.097714	-0.006207
33,34	0.00003352	2.449569	-0.277033	-0.017997
35,36	0.00179097	1.913633	-0.127583	-0.010610
37,38	0.00010250	1.856931	-1.116372	-0.095248
39,40	0.00459397	1.260021	-0.025866	-0.003267
41,42	0.00157342	1.232018	-0.150042	-0.019379
43,44	0.00002596	0.626456	-0.236758	-0.060041
45,46	0.00078983	0.047023	-0.198318	-0.557319
47,48	0.00460625	0.935691	-5.853981	-0.705590
49	0.00008506	-0.000000	-22.241012	-1.000000

5.3 Discussion

It is shown that the solution and contribution factors obtained by the proposed approach are closest to the true solutions. In this sub-section, the difference in contribution factors as described above, is discussed.

The contribution factors σ_{ij} , $\sigma_{ij}^{\mathbf{1}}$, $\sigma_{\mathbf{2}im}$, $\sigma_{ik}^{\mathbf{2}}$, $\sigma_{\mathbf{22}ikl}$ and Prony's results in the above case studies are corresponding to the following eigenvalues respectively:

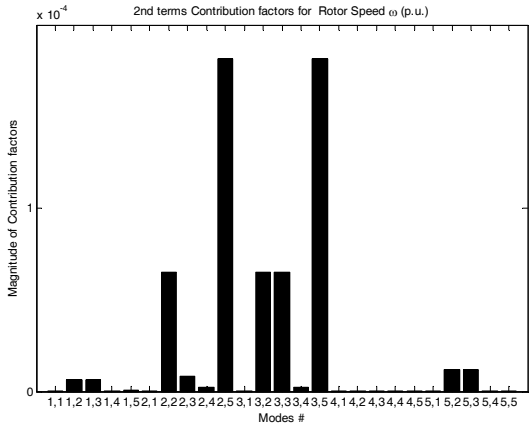

Fig. 13. The distribution of contribution factors $\sigma_{ik}^{\mathbf{2}}$ of ω in SIMB

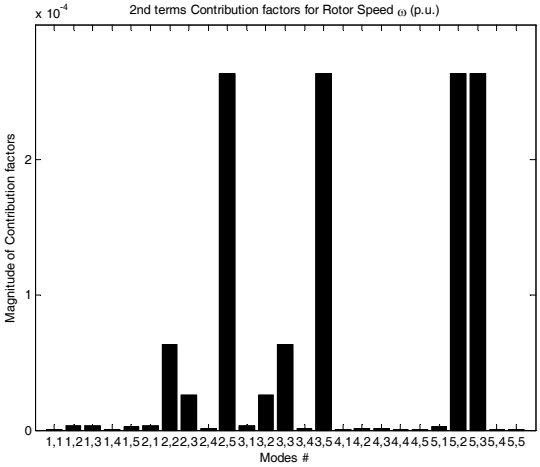

Fig. 14. The distribution of contribution factors $\sigma_{\mathbf{22}ikl}$ of ω in SIMB

$$\lambda^{\mathbf{1}} = [\lambda_1, \lambda_2, \cdots, \lambda_n]$$

$$\lambda^{\mathbf{2}} = \left[\underbrace{\mathbf{2}\lambda_1, \lambda_1 + \lambda_2, ..., \lambda_1 + \lambda_n}_{n-times}, \underbrace{\mathbf{2}\lambda_2, \lambda_2 + \lambda_3, ..., \lambda_2 + \lambda_n}_{(n-\mathbf{1})times}, \right.$$

$$\left. \underbrace{\mathbf{2}\lambda_3, \lambda_3 + \lambda_4, ..., \lambda_3 + \lambda_n}_{(n-\mathbf{2})times}, \cdots, \underbrace{\mathbf{2}\lambda_n}_{\mathbf{1}-times} \right]$$

That is to say, the contributions of the $\lambda_{ij}^{\mathbf{2}}$ and $\lambda_{ji}^{\mathbf{2}}$, that should be equal in general, are combined. According to different methods in handling $\lambda_{ij}^{\mathbf{2}}$ and $\lambda_{ji}^{\mathbf{2}}$ separated, the distribution of $\sigma_{ik}^{\mathbf{2}}$, $\sigma_{\mathbf{22}ikl}$ of ω in SIMB are shown in Fig. 13 and Fig. 14 respectively.

In Fig. 13, it is visually seen that the contribution factor $\sigma_{\mathbf{2,5}}^{\mathbf{2}}$ is not equal to $\sigma_{\mathbf{5,2}}^{\mathbf{2}}$, and such condition appears in the distribution of all contribution factors. On the contrary, the contribution factor $\sigma_{\mathbf{22}i(\mathbf{2,5})}$ is equal to $\sigma_{\mathbf{22}i(\mathbf{5,2})}$ as in Fig. 14. Actually $\sigma_{\mathbf{22}ikl} = \sigma_{\mathbf{22}ilk}$ in the whole distribution. The solutions obtained by the Carleman linearization are

not as good as that by the Poincaré-like Carleman linearization method because the structure of Carleman linear solution violates the interactional equivalence of $\sigma_{ij}^2 = \sigma_{ji}^2$.

6. Conclusion

The advantage embedding technique is that it replaces the original system with an equivalent system by embedding the new state variables and their differential equations. Hence, linear methods can be directly applied to solve the system. However, due to the neglected part of nonlinear information in the truncated Carleman linearization, it does not perform well in the modal analysis of power system, especially in the analysis of nonlinear modal interaction. In this paper, the Poincaré transfor-mation approach combined with Carleman embedding technique is introduced to improve the performance of analysis in power system, especially, all the nonlinear information is included.

The numerical simulations verify the effects of the improved approach by comparing the approximate curves (the linear solution, the linear-Carleman solution and the P-Carleman solution) with the true response, as well as their contribution factors. Simulation results demonstrate that the combined approach can get much better results. The proposed approach improves the performance, hence more accurate results can be obtained, by avoiding the asymmetry in handling the contribution factors.

Appendix
Poincaré Transformation

In this appendix, the Poincaré Transformation is briefly introduced from the pure mathematics, detailed in [7].

A. General setting

Consider the formal vector-valued power series

$$\dot{x} = Ax + f_2(x) + f_3(x) + \cdots = Ax + \sum_{k=2}^{\infty} f_k(x) \quad x \in R^n, \quad f: R^n \to R^n \tag{A-1}$$

in n variables with complex coefficients.

where, $f_k(x)$ is homogeneous of order $(k+1)$ in the x. A is the canonical form of the the original vector field.

B. Poincaré theorem and its transformation

The following theorem is the fundamental result of Poincaré's dissertation.

Poincaré Theorem. *If the eigenvalues of the matrix A are nonresonance, the equation*

$$x = Ax + \cdots \tag{A-2}$$

can be reduced to a linear equation

$$\dot{y} = Ay \tag{A-3}$$

by a formal change of variable $x = y + \cdots$ (*the dots denote series starting with terms of degree greater than one, i.e.* $h_k(y)$, k=2,3,….).

The identity changes of coordinates are also called *Poincaré Transformations*.

C. Transformation to poincaré normal form

Substitute the Poincaré transformation $x = y + \sum h_k(y)$ into the Eq. (A-2), and denote by $D = \partial/\partial y$ the differential operator.

$$\dot{y} = [I + Dh_k(y)]^{-1}\{Ay + A\sum_{k=2}^{\infty} h_k(y) + \sum_{k=2}^{\infty} f_k(y)\} \tag{A-4}$$

Provided the $[I+Dh_k(y)]$ is invertible and approximated by

$$[I + Dh_k(y)]^{-1} = I - Dh_k(y) + (Dh_k(y))^2 + \cdots \tag{A-5}$$

Substituting (A-6) into (A-5), one can get the result,

$$\dot{y} = Ay + \sum_{k=2}^{\infty} \hat{f}_k(y) \tag{A-6}$$

where, $\hat{f}_k(y) = f_k(y) + Ah_k(y) - Dh_k(y)y$.

It is clear that the ideal simplification would be to take h_k so that

$$Dh_k(y)y - Ah_k(y) = f_k(y) \tag{A-7}$$

a substitution which would remove the terms of order k from the vector field. The vectors $h_k(y)$, $k \geq 3$ may be determined from the solution of the homological equation

$$L_A(h_k(y)) = Dh_k(y)y - Ah_k(y) \tag{A-8}$$

where, the linear operator L_A converts every field into the linear fields $Dh_k(y)y - Ah_k(y)$. h_k is the unknown and the right expression is the known vector field. One should note that this is a problem of linear algebra.

Denote by e_i an eigenvector of A with eigenvalue λ_i. $\{e_1, e_2 \cdots e_n\}$ be a standard basis for the coordinates $(y_1, y_2 \cdots y_n) \in R^n$. Let the eigenvectors of L_A are the vector-valued monomials $h_k(y) = (y_1^{m_1}, y_2^{m_2}, \cdots, y_n^{m_n})e_i$ of degree $\sum m_l = k$, which form a basis for the finite dimensional vector space H_k of all valued polynomials of precise degree k. If A is diagonal, the eigenvalues of L_A depend linearly on the eigenvalues of A,

$$L_A y^m e_i = [\sum_{l=1}^{n} m_l \lambda_l - \lambda_i] y^m e_i \quad \text{(A-9)}$$

Thus, the operator L_A is also diagonal. The unknown h_k can be obtained from the following

$$[\sum_{l=1}^{n} m_l \lambda_l - \lambda_i] h_k(y) = f_k(y) \quad \text{(A-10)}$$

Therefore, if $\sum_{l=1}^{n} m_l \lambda_l - \lambda_i \neq \mathbf{0}$, the terms of order k in (A-7) can be removed from the vector field. The Eq. (A-7) can be transform into linear equation,

$$\dot{y} = Ay \quad \text{(A-11)}$$

Finally, the solution of the original equation with initial value $x_0 = Uy_0$, the eiginvalues λ_j and $h_k(y)$, can be written as

$$x = \sum_{j=1}^{n} u_{ij} y_0 e^{\lambda_j t} + \sum_{k=2}^{\infty} \frac{f_k(y)}{\sum_{l=1}^{n} m_l \lambda_l - \lambda_i} \quad \text{(A-12)}$$

where, $u_{ij} \in U$.

Acknowledgements

This work was supported in part by Natural Science Foundation of China (NFSC, Grant No. 50977007) and Doctoral Fund of Ministry of Education of China (RFDP, grant no. 20090185110018)

References

[1] J. J. Sanchez-Gasca, V. Vittal, M. J. Gibbard et al, "Inclusion of higher order terms for small-signal (modal) Analysis: committee report-task force on assessing the need to include higher order terms for small-signal (*modal*) analysis," IEEE Trans. Power Systems, Vol. 20, No. 4, pp. 1886-1904 , Nov. 2005.

[2] Huang Qi, Wang Zhouqiang, Zhang Changhua, "The third order analytical solution of power systems based on *normal* form," Journal of UESTC, Vol. 38, No. 6, pp. 957-961, Nov. 2009.

[3] H. M. Shanechi,, N. Pariz, and E. Vaahedi, "General nonlinear modal representation of large scale power systems," IEEE Trans. Power Systems, Vol. 18, No. 3, pp. 1103-1109, August 2003.

[4] Krzysztof Kowalski, Willi-Hans Steeb, Nonlinear Dynamical Systems and Carleman Linearization: Singapore: World Scientific Publishing Co. Pt. Ltd., 1991, p. 75-94.

[5] Filippo Cacace, Valerio Cusimano, Alfredo Germani, "An efficient approach to the design of observers for continuous-time systems with discrete-time measurements," The 50th IEEE Conference on Decision and Control and European Control Conference (CDC-ECC), December 12-15, 2011, Orlando, FL, USA.

[6] J. Arroyo, E. Barocio, R. Betancourt, and A. R. Messina, "A bilinear analysis technique for detection and quantification of nonlinear Quantification of Nonlinear Modal Interaction," *IEEE Power Engineering Society General Meeting*, June 18-22, 2006, Montreal Quebec, Canada.

[7] V. I. Arnold, *Geometrical methods in the theory of ordinary differential equations,* 2nd ed: New York: Springer-Verlag, 2004, p. 180-221

[8] Zhang Xianda, *Modern Signal Processing* .2nd edition. Beijing: Tsinghua University Press, 2006, pp. 119-125

[9] Shu Hongchun, *Application of signal processing in electrical engineering*: Beijing Science Press, 2009

[10] P. Kundur. *Power System Stability and Control*: McGraw-Hill, 1994. p. 732.

[11] Z. Wu, X. Zhou, "Power System Analysis Software Package (PSASP)-an integrated power system analysis tool," *Proc. International Conference on Power System Technology*, Vol.1, 1998, pp: 7-11.

[12] Wang Xifan, *Modem power system analysis*: Beijing Science Press, 2003, p. 326-327.

Zhou-qiang Wang was born in Sichuan Province in the People's Republic of China. He received the B.S. degree in automation from Shanxi University, Shanxi, China, in 2005, and MS degree from University of Electronic Science and Technology of China (UESTC), Chengdu, Sichuan, China, in 2009. He is currently pursuing the Ph.D. degree at UESTC. His current research includes power system stability, monitoring and control.

Qi Huang was born in Guizhou Province in the People's Republic of China. He received his BS degree in Electrical Engineering from Fuzhou University in 1996, MS degree from Tsinghua University in 1999, and Ph.D. degree from Arizona State University in 2003. He is currently a professor at University of Electronic Science and Technology of China (UESTC) and the Deputy Dean of School of Energy Science and Engineering, UESTC, and the Director of Sichuan State Provincial Lab of Power System Wide-area Measurement and Control.

Chang-hua Zhang (M09) was born in Hubei province in the People's Republic of China. He received the Diploma degree invehicleengineer- ing from Wuhan University of Science and Technology, Wuhan, China, in 1993, the M.Sc. degree in vehicleengineering from Wuhan University of Technology, Wuhan, China, in 2004, the Ph.D. degree from Institute of Automation Chinese Academy of Sciences in 2007. He is currently an associate professor at the School of Energy Science and Technology of University of Electronics Science and Technology of China (UESTC) and a visiting scholar of Loughborough University, UK. He is an IEEE member since 2009. His current research and academic interests include the smart grid, power market, and microgrids.